Single Axis Piezoceramic Gimbal

Garnett Horner[a] and Barmac Taleghani[b]

[a]NASA Langley Research Center, MS 230, Hampton VA 23681

[b]U.S. Army Vehicle Technology Center, Hampton, VA

ABSTRACT

This paper describes the fabrication, testing, and analysis of a single axis piezoceramic gimbal. The fabrication process consists of pre-stressing a piezoceramic wafer using a high-temperature thermoplastic polyimide and a metal foil. The differential thermal expansion between the ceramic and metal induces a curvature. The pre-stressed, curved piezoceramic is mounted on a support mechanism and a mirror is attached to the piezoceramic. A plot of gimbal angle versus applied voltage to the piezoceramic is presented. A finite element analysis of the piezoceramic gimbal is described. The predicted gimbal angle versus applied voltage is compared to experimental results.

Keywords: actuator, gimbal, piezoceramic, scanner

INTRODUCTION

The development of a new processing technique called THUNDER (THin-layer composite UNimorph piezoelectric Driver and sEnsoR) technology[1] enables new types of actuator concepts. The THUNDER technology produces a curved piezoceramic by combining a flat piezoceramic wafer with a thin metal foil using a polyimide thermoplastic called LARC-SI as an adhesive. Using a thin film of the LARC-SI between the metal foil and the piezoceramic, the three are held together using pressure while they are heated above the melting point of the LARC-SI to produce a composite. As the composite is cooled below the melting point of the LARC-SI, the foil is bonded to the piezoceramic. Upon further cooling, the miss-match in coefficient of thermal expansion between the metal foil and the ceramic causes a compressive pre-stress to exist in the piezoceramic when the composite returns to room temperature.

This curved composite using THUNDER technology produces large amplitudes of motion when a voltage field is applied across the piezoceramic. Depending upon the polarity of the applied field, the radius of curvature of the composite will either increase or decrease. When mechanisms are coupled to the composite along the axis of symmetry, translational motion is achieved as the applied field is varied.

The subject of this paper is to investigate an approach to produce rotational motion using THUNDER technology. Our vision is to develop a simple piezoelectric gimbal that does not have any moving parts such as would be found in a mechanism. This piezoceramic gimbal would be used with a small mirror to produce a scanner for applications to sampling or surveillance-type instruments on spacecraft.

1. THE CONCEPT

The concept used herein for transforming the linear motion of the usual THUNDER technology developed composite into rotational motion is simple and straightforward. We note that the radius of curvature of a single THUNDER technology piezoceramic composite changes with applied voltage field. This is shown schematically in Figure 1.

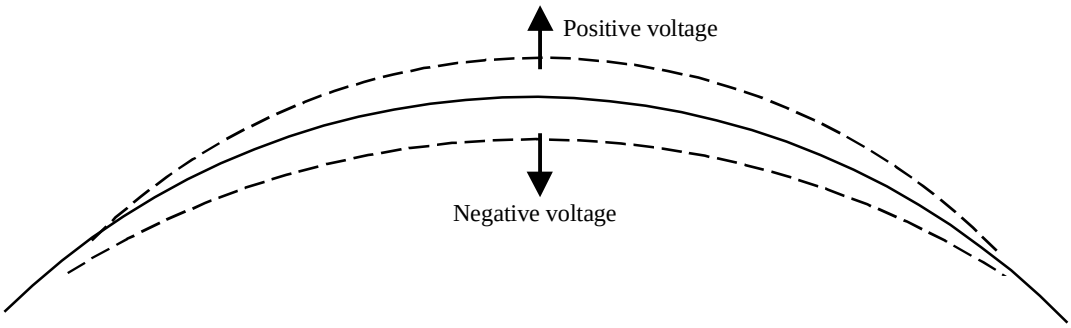

Figure 1: Changes in curvature of THUNDER wafer with free-free boundary conditions

We suggest that if the increased and decreased changes in curvature could be combined into a single composite, the axis of symmetry would rotate instead of translating. This rotational axis would produce an angular motion that could be used as a gimbal actuator for a device such as a scanning mirror.

As shown in Figure 2, starting with an unelectroded piezoceramic wafer such as PZT-5A, an identical electrode pattern is screened onto both sides of the ceramic. The screening process uses a mask and silver paste to apply the electrode pattern. As shown in Figure 2 there are two electrode surfaces and on the opposite side there is an identical electrode pattern. These four electrode surfaces constitute two independent piezoceramic actuators. Since the electrode surfaces are equal in area, there are two separate actuators on a single piezoceramic wafer.

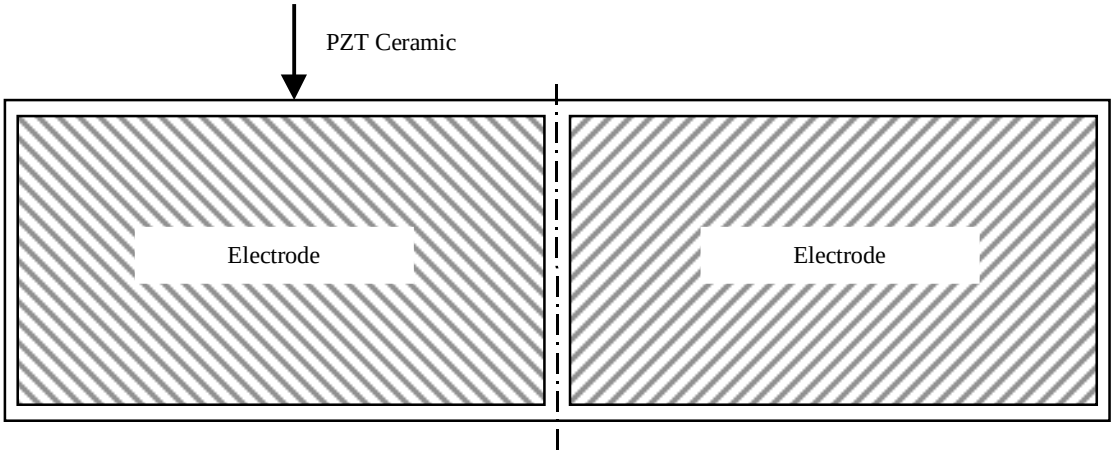

Figure 2: Electrode pattern

The process for fabrication of this gimbal is similar to that used to process THUNDER technology piezoceramics. A .008" thick electroded PZT-5A ceramic as shown in Figure 2 is bonded to a .002" thick sheet of stainless steel using a polyimide thermoplastic. The bonding or consolidation of these pieces is done in an autoclave at elevated temperatures and pressures. As the autoclave is cooled, the thermoplastic adhesive bonds but since there is a mismatch in the coefficient of thermal expansion (CTE) between the PZT ceramic and the stainless steel, the consolidated assembly is curved due to different thermal strains in the ceramic and metal. A consolidated assembly with electrical leads attached is shown in Figure 3.

Figure 3: Consolidated, pre-stressed piezo-metal composite

As shown in Figure 4, after consolidation, the curved piezo-metal composite is bonded to a polypropylene mount and a mirror is bonded in the center. The polypropylene has good fatigue properties which allows the mount to be made from a single sheet of the polypropylene and a mechanism was formed by making partial cuts in the material along the desired hinge axis. Polypropylene was chosen because of its good fatigue properties. Next, each half of the ceramic is poled in the same direction by applying 500 volts D.C.

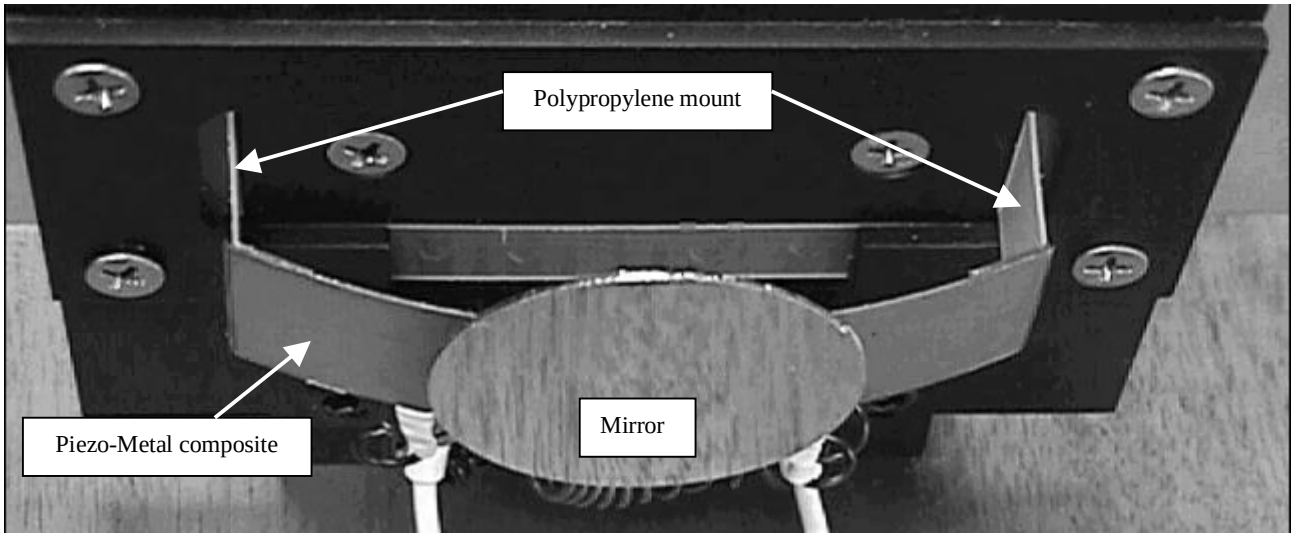

Figure 4: Piezo-metal composite with mirror

The piezoceramic halves are connected such that the positive side of one half is connected to the negative side of the other half. The negative side of the first half and the positive side of the second half are connected to an amplified voltage source. In this way, one amplifier can be used to drive the two halves in the opposite sense. That is, as one half is becoming more domed and shorter, the other half is becoming flatter and longer. This combination of motions causes the mid-point between the two piezoceramics to rotate. This mid-point rotation can be used to command and control the mirror gimbal angle.

2. TEST RESULTS

The gimbal angle was measured as a function of the applied voltage using the setup shown in Figure 5. The light source is reflected off of the mirror onto a detector that measures a translational distance, s, along the detector. Knowing the distance, r, from the mirror to the detector and using a small angle approximation, the gimbal angle is simply s/(2r), that is, half the reflected beam angle.

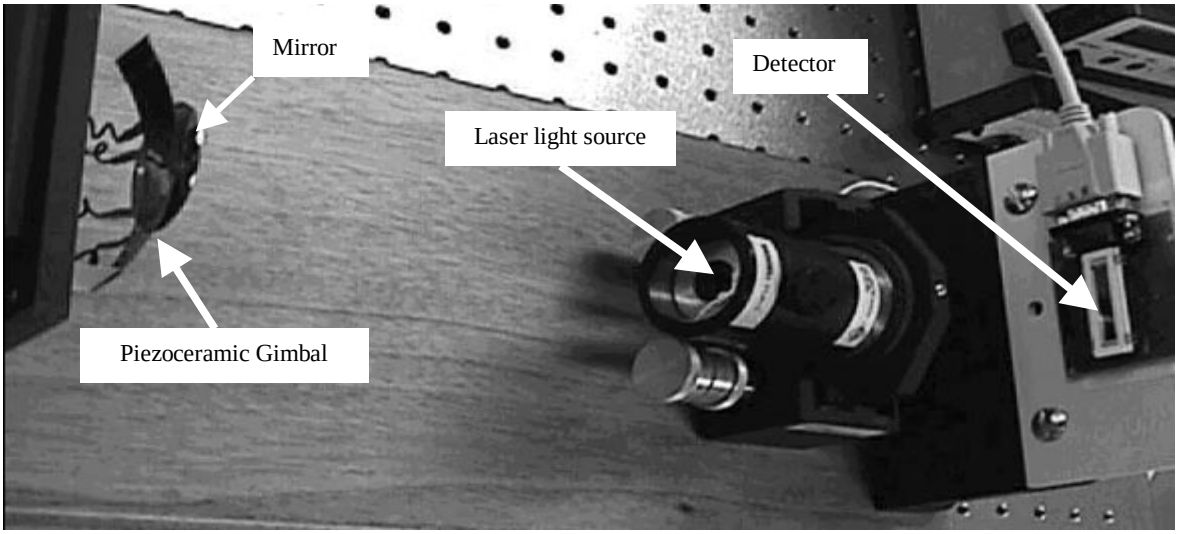

Figure 5: Experimental set-up for measuring gimbal angle as a function of driving voltage

Using a data acquisition system, the driving voltage to the piezoceramic and the corresponding location of the beam on the detector are stored for several repeated cycles. The driving voltage was varied between ±200 volts at nearly quasi-static conditions. The results of this test are shown in Figure 6. As seen from the hysteresis, the composite piezoceramic gimbal is non-linear and dissipative. This is likely due to several factors. First, the piezoceramic is a sintered material which will likely exhibit micro-level motion between adjacent particles. Second, the polymer used to bond the metal foil to the piezoceramic could have some dissipation. From the data, the gimbal angle varies between -0.64 to 1.18 degrees. Nominally, this is ±0.91 degrees.

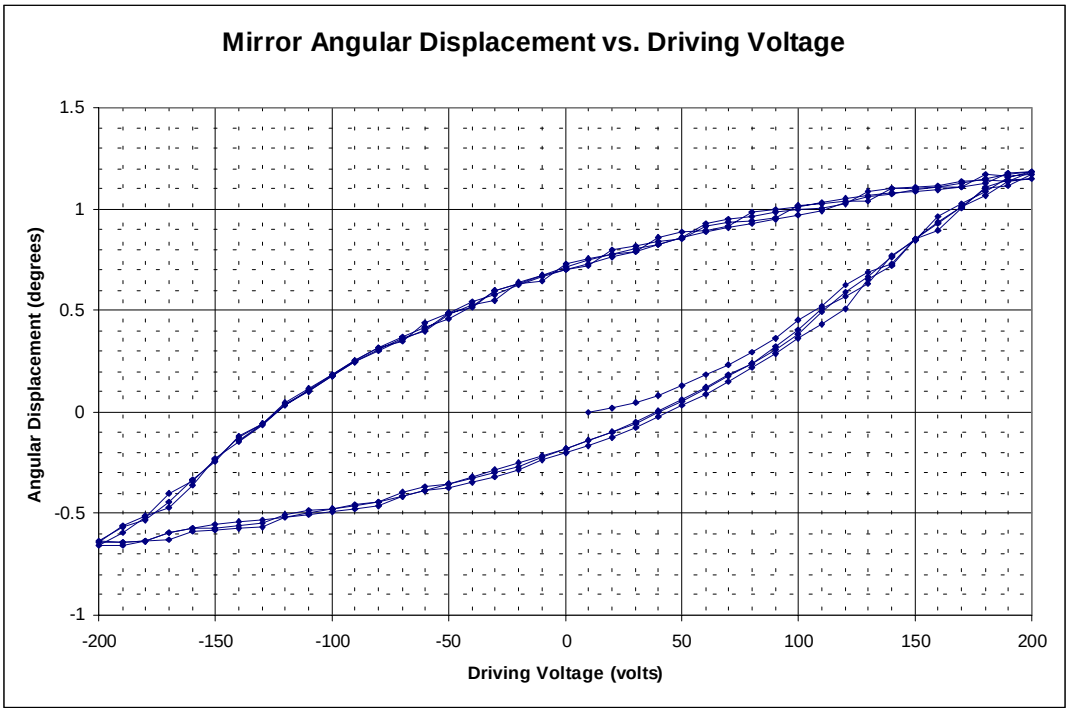

Figure 6: Gimbal angle (Angular displacement) as a function of driving voltage

3. ANALYSIS

3.1 Modeling Approach

A NASTRAN[2] non-linear finite element model was developed for predicting dome heights resulting from fabrication and applied voltages to the PZT layer. The finite element model assumes that all layers are bonded at the glass transition temperature of LARC-SI (assumed to be 250 degrees C). The bonding constrains all layers to move together while the specimen is cooled, thus generating thermal stresses due to differing CTEs in the layers. This bonding was modeled by attaching the layers together using rigid bars. The model only accounts for the process when the device was cooled from 250 degrees C to room temperature (25 degrees C).

The model is divided into two parts. The first part models the fabrication process from the glass transition temperature to room temperature where the initial doming occurs. The thermal strain resulting from cooling is calculated as follows,

$$\varepsilon_{thermal} = \alpha \Delta T \tag{1}$$

where $\varepsilon_{thermal}$ is the thermal strain due to the cooling process, α is the coefficient of thermal expansion, and ΔT is the temperature difference.

The second part models the strain resulting from the applied voltage, which is determined as follows,

$$\varepsilon_{piezo} = d_{31} \frac{V}{t_{pzt}} \tag{2}$$

where ε_{piezo} is the piezoelectric strain, d_{31} is the piezoelectric charge constant, V is the applied voltage, and t_{PZT} is the thickness of the PZT layer.

To incorporate the voltage effects into the NASTRAN model, a simple thermal analogy was used. The piezoelectric charge constant d_{31} divided by the PZT ceramic thickness was an equivalent coefficient of thermal expansion, and voltage is equivalent to a temperature difference. That is,

$$V \propto \Delta T \tag{3}$$

and

$$\frac{d_{31}}{t_{pzt}} \propto \alpha \tag{4}$$

The total strain is given by

$$\varepsilon_{total} = \varepsilon_{piezo} + \varepsilon_{thermal} \tag{5}$$

3.2 Model description

The model geometry was developed and meshed using I-DEAS[3] Master Series Version 6.0. Creating all the layers and stacking them developed the 3D-geometry model. A mid-surface was then created on each layer for elements to be placed. After meshing was completed, the mid-surfaces were connected using rigid bars as shown in Figure 7.

The NASTRAN model consists of 4 layers consisting of stainless steel, polyimide, PZT 5A, and polyimide. These layers correspond to the actual hardware lay-up. The material properties and the lay-ups are shown in Table 1. The model includes 330 CQUAD4 quadrilateral plate elements, 315 rigid elements RBAR's, 420 nodes, and 1500 degrees-of-freedom. The assumed boundary conditions for the model are pinned at one end and guided at the other end. SOL 106 was used for non-linear static thermal analysis. To assure convergence, the temperature range was divided into ten segments. There have not

been any measurements of d_{31} for the prestressed ceramic. An assumed value for d_{31} = - 6.9(10)$^{-9}$ inches/volt, the piezoelectric charge constant, was used.

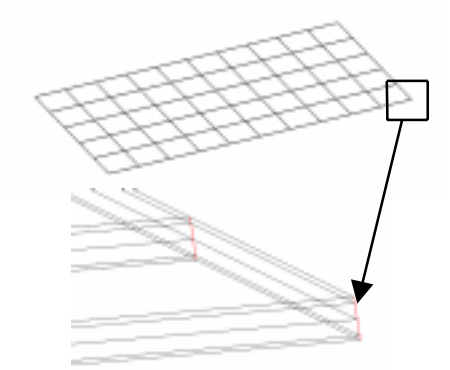

Figure 7. Rigid Bars

The assumption was made that at 250 degrees C the layers are bonded and consolidated. Therefore, the cooling process was modeled from 250 degrees C to 25 degrees C. RBAR's were used to model this bonding. Since RBAR's were connected together, there exist independent and dependent degrees of freedom on nodes connected by RBAR's. The nodes on the stainless steel mid-layer had the independent degrees of freedom, and all the nodes on other layers had the dependent degrees of freedom. TEMP (INIT) and TEMP (LOAD) were used to assign initial and final temperature loads to TEMPD cards. The model included two subcases. The initial part modeled the fabrication cooling process. The second part keeps all of the grid points at room temperature, while voltages (as equivalent temperatures) were added to nodes on the PZT layer by using TEMP cards. Upon completion of the NASTRAN analysis, the results were exported to I-DEAS for graphical presentation.

	Material	Thickness (in.)	Modulus of Elasticity (E) (psi) x10^6	Coefficient of Thermal Expansion(CTE) $10^{-6}/^0C$
Layer 1	LARC-SI	0.001	0.58	46
Layer 2	PZT 5A	0.0068	9	1.5
Layer 3	LARC-SI	0.001	0.58	46
Layer 4 (Bottom layer)	Stainless Steel	0.002	38	17.3

Table 1: Lay-ups and Material Properties used in NASTRAN Non-linear model

3.3 Analysis results

The rotation of the center nodes, shown in Figure 8, was used to calculate the rotational angle of the gimbal. The model clearly displayed the expected S shape curve of the gimbal when loads were applied. The calculated angles of the peak rotation for the center nodes were between 2.8 and 3.3 degrees. Figures 9 and 10 show plots of angles of rotation versus applied voltage for the center nodes.

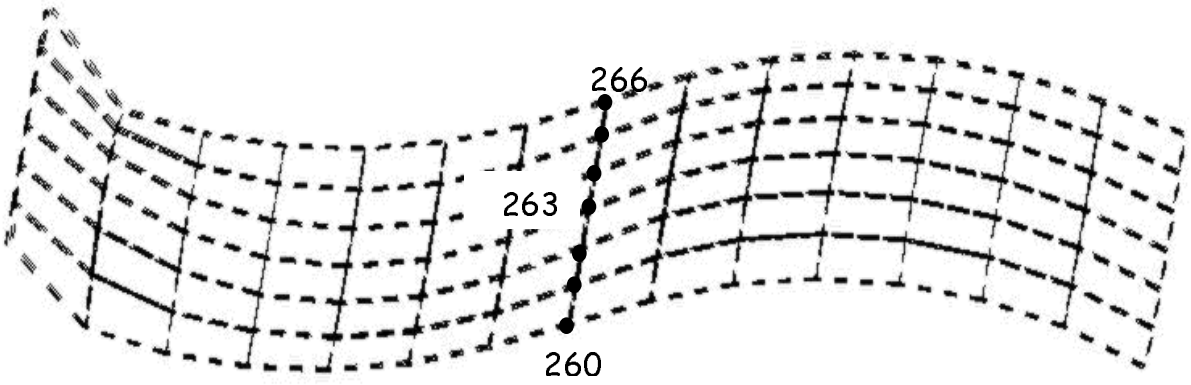

Figure 8: Deflection of FEM grid points from curved shape

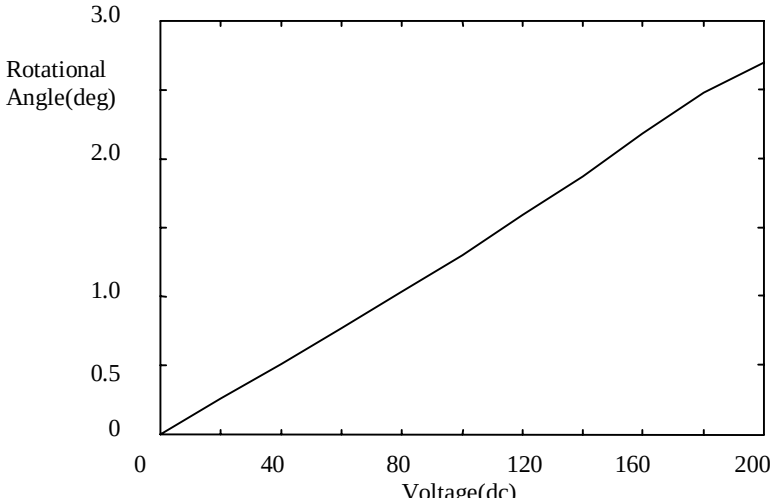

Figure 9: Rotation at node 260 & 266 vs. driving voltage

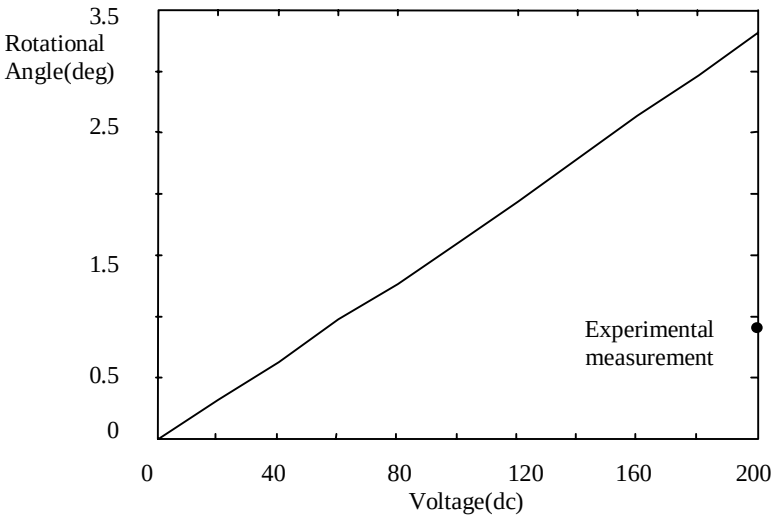

Figure 10: Rotation at node 263 vs. driving voltage

4. ANALYSIS VS. TEST RESULTS

From the results in Figures 9 and 10, the relationship between the rotational angle and the voltages is almost linear. The lowest rotational angle, 2.8 degrees, as seen in Figure 9 occurs at nodes 260 and 266. The largest rotation angle, 3.3 degrees, occurred at the center, node 263. The analysis predicted a gimbal angle of ±3.3 degrees for a driving voltage of ±200 volts. The experimental measurements of the gimbal angle give approximately ±1.0 degree for ±200 volts. In general, the analytical model is more flexible than the actual hardware and over-predicts the results. There could be several factors contributing to this discrepancy. First, the polypropylene support for the piezoceramic composite has a non-ideal hinge at both ends that support the curved piezoceramic composite. This non-ideal hinge has friction and stiffness and thus the boundary conditions are not ideal. The FEM has pinned boundary conditions while the actual hardware deviates in such a way as to increase the boundary stiffness. Secondly, the actual piezoceramic composite is thicker than the FEM at several locations because of the thickness of the electrical leads. Thirdly, the FEM does not model the material damping that gives rise to the hysteresis loop in the actual response data. The material damping will cause the response to be less than the undamped analysis prediction. Not having an accurate value of d_{31} and using an estimate also contributes to the analysis predicting more rotation than the test.

5. CONCLUDING REMARKS

This paper describes the fabrication, testing, and analysis of a single axis piezoceramic gimbal. The fabrication process consists of pre-stressing a piezoceramic wafer using a high-temperature thermoplastic polyimide and a metal foil. The differential thermal expansion between the ceramic and metal induces a curvature. The pre-stressed, curved piezoceramic is mounted on a support mechanism and a mirror is attached to the piezoceramic. A plot of gimbal angle versus applied voltage to the piezoceramic is presented. A finite element analysis of the piezoceramic gimbal is described. The predicted gimbal angle versus applied voltage is compared to experimental results.

In general, better correlation between experiment and prediction should be achievable. This may require improved modeling approaches as well as better hardware implementations. Hopefully, as research continues to improve upon the hardware and model approach, better correlation will be reached and results will be reported at that time.

The feasibility of a piezoceramic scanner has been demonstrated and has promise as a high frequency scanner. In general, piezoceramics can achieve high frequency response and it is anticipated that this scanner will, also. When the model is upgraded, the scanner design can be optimized for dynamic response at high frequencies. Traditional gimbals are mechanisms with bearings or flexures driven by motors. The piezoceramic gimbal is simple, be inexpensive to manufacture, has no parts to wear out, and is lightweight.

ACKNOWLEDGEMENTS

The authors wish to thank Mr. Ruben Remus of NASA Langley for his work with the data acquisition system and Messrs. John Teter, Eugene Robbins, and Ben Copeland of NASA Langley for the design and fabrication of the piezoceramic gimbal.

REFERENCES

1. K. M. Mossi, G. V. Selby, and R. G. Bryant, “Thin-layer Composite Unimorph ferroelectric driver and sensor properties.” Materials Letters, 35 (1998) 39-49.

2. L. H. Sang, MSC / NASTRAN Handbook for Non-Linear analysis, The MacNeil Schwendler Corporation, 1992.

3. I-DEAS Simulation User’s Guide, Structural Dynamics Research Corporation, 1996.